Improving efficiency of LNOI terahertz waveguide via geometry optimisation

Yu Youyou, supervised by Dr. Stephanie Adeyemo
University of Cambridge

September 16, 2025

1 Introduction

Today, increasingly densely populated cities are becoming more vulnerable to the spread of infectious diseases. The COVID-19 pandemic, which stretched global health systems to their limits, highlighted the urgent need for advanced and non-invasive diagnostic tools capable of detecting infections and diseases in the early stages. Terahertz (**THz**) sensing offers great potential for rapid virus screening and health diagnostics [1]. THz waves penetrate many optically opaque materials, and unlike X-rays and gamma rays, have low photon energies [2], making them ideal for non-invasive biological particle detection.

However, THz waves are highly susceptible to molecular absorption, which means they suffer significant attenuation in the air [4]. Developing highly sensitive detectors with low signal-to-noise ratio (SNR) for weak THz signals is therefore essential to reliable and effective application of this technology. Thin-film lithium niobate on insulator (LNOI) waveguides have emerged as a novel approach to developing highly sensitive THz detectors as LNOI offers unprecedented properties for electro-optic (EO) detection, including large EO coefficient, high linearity, and especially its potential for good phase matching between THz E-field and near-IR probe waves which extracts information about terahertz waves via EO effect [5].

Detector geometry plays an important role in maximising efficiency. Waveguide geometry parameters such as LNOI film thickness, modulator length and spacing directly affects phase matching between the optical and THz fields over the propagation length, as well as good optical confinement within LNOI film[6]. Good phase matching is especially critical for detecting weak THz signals because it maximizes EO interaction by ensuring continuous energy transfer between the optical and THz fields over the propagation length, conserving signal strength. Good optical confinement of the near-IR probe wave within LNOI film influences detection efficiency by controlling field overlap and propagation losses.

This project aims to investigate the optimal geometric parameters of electrode-less LNOI waveguides to achieve both good optical confinement and good phase matching, thereby contributing to the development of highly sensitive and efficient THz sensing technology for healthcare applications.

2 Related Work

Prior work on lithium niobate (LN) waveguides has established the feasibility of electrode-less electro-optic (EO) sensing. Gutiérrez-Martínez et al. [3] modeled and experimentally characterized LN waveguides used as dielectric field sensors, showing that EO response can be achieved without electrodes, a principle central to this project. More recently, Wilke et al. [5] demonstrated a thin-film LN EO THz detector, validating the practicality of LNOI-based detection with near-infrared probes and providing a baseline setup on which this research builds.

Much of the design literature has focused on modulators, but their analysis of geometry remains directly relevant. Studies on high-speed and optimized LNOI modulators provided calculation approaches for refractive index change (Δn) and revealed how parameters such as film thickness, ridge width, and electrode spacing affect confinement and the voltage-length product ($V\pi L$). Work on LN slot waveguides further highlighted how slot width and thickness control effective index and cutoff conditions, pointing to geometry as the dominant factor in balancing confinement with phase matching.

Unlike the more common Mach–Zehnder interferometers, this project leverages the intrinsic birefringence of LNOI for phase matching, an underexplored approach. This project also works with electrode-less LNOI waveguides, which minimally disturbs the electric field and more sensitive to signal [3]. Building on these insights, the research investigates geometric optimization of electrode-less LNOI waveguides to achieve both strong confinement and efficient phase matching for highly sensitive THz detection.

3 Method

3.1 Detection Scheme

The electro-optic modulation (EOM) mechanism relies on the Pockels effect, where an applied electric field induces a change in the refractive index of a material. When a voltage is applied across a lithium niobate waveguide, the refractive index change is proportional to the applied electric field E_z. This modifies the effective index of the optical mode, which can be expressed as:

$$\Delta n_{\text{eff}} = \frac{1}{n_{\text{eff}}} \frac{\iint_{LN} n(x,z)\, \Delta n(x,z)\, |E_0(x,z)|^2 \, dx\, dz}{\iint_{\infty} |E_0(x,z)|^2 \, dx\, dz} \tag{1}$$

Here:

- $n(x,z)$ is the refractive index distribution of the material.
- $\Delta n(x,z)$ is the refractive index change induced by the Pockels effect at position (x,z).
- $E_0(x,z)$ is the optical mode field distribution in the waveguide.
- n_{eff} is the effective refractive index of the optical mode.

The numerator integrates only over the lithium niobate region, where the Pockels effect modifies the refractive index. The denominator integrates over the entire waveguide cross-section, normalizing the optical mode power.

To obtain the specific local perturbation in the refractive index, we use the following:

$$\Delta n = \Delta n_e = -\frac{1}{2} n_e^3 \gamma_{33} E_z \tag{2}$$

where

- n_e is the unperturbed extraordinary refractive index
- γ_{33} is the relevant electro-optic coefficient
- E_z is the applied electric field along the crystal axis.

Utilising this phenomenon, the set up as shown in figure 1 is simulated. The incoming optical beam ($\omega = 800nm$) is polarised at 45° to the ordinary optical axis of the thin film lithium niobate crystal. The substrate is made of SiO_2 This polarization was electro-optically modulated by the terahertz field incident on the LN crystal. Hence, the optical beam polarisation varies as the terahertz electric field signal varies, allowing the signal to be obtained accordingly.

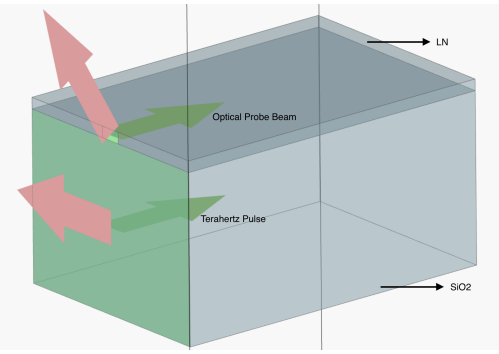

Figure 1: Thin Film LN waveguide

3.2 Optical confinement

Optical confinement in lithium niobate (LN) films is crucial because it ensures strong overlap of the optical mode with the active material, maximizing electro-optic interactions. Strong confinement reduces optical loss to the substrate or cladding, allowing compact devices with higher efficiency. It also enables better control over dispersion and phase matching, which is key for integrated photonics applications. In this project, modes in the lithium niobate thin film are simulated by solving Maxwell's equations using the finite element method (FEM) and finite-difference time-domain (FDTD) techniques on the Tidy3D platform at the operating wavelength of 800 nm. The solvers produced mode profiles, from which the effective refractive index n_{eff} was extracted as the eigenvalue associated with the propagation constant. Mode confinement was quantified by integrating the optical field intensity in the LN region relative to the total field, expressed as a confinement factor

$$\Gamma = \frac{\iint_{\text{LN}} |E(x,z)|^2 \, dx \, dz}{\iint_{\infty} |E(x,z)|^2 \, dx \, dz},$$

which was compared across varying geometries to optimize guiding performance.

3.3 Phase matching

In this project, Cherenkov phase matching is employed because it provides a simple and efficient way to phase match the terahertz waves propagating in SiO_2 substrate and optical probe beam in lithium niobate (LN) films without requiring periodic poling or extremely precise domain engineering.
In this project, Cherenkov phase matching is realized by tailoring the lithium niobate (LN) film geometry so that the optical mode at $\lambda = 800$ nm has an effective index equal to the phase index of the emitted THz wave in the substrate. The Cherenkov angle β is set by the velocity (or index) mismatch:

$$\cos\beta(\Omega) = \frac{v_{\text{opt}}}{v_{\text{THz}}} = \frac{n_{\text{eff}}(\lambda = 800 \text{ nm})}{n_{\text{THz}}(\Omega)}.$$

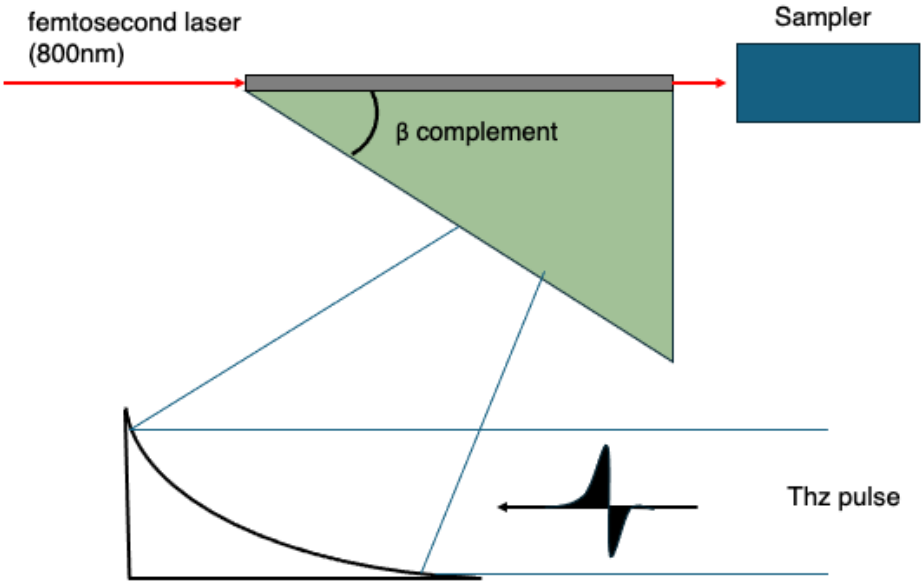

Figure 2: Enter Caption

Mode properties and confinement were obtained using FDTD simulations on the Tidy3D platform. Parameter sweeps of film thickness, width, etch depth, and cladding materials were performed. As geometries are varied, the mode solver used to calculate optical and THz eigenmodes and their effective indices. A custom written simulator is used while to validated the polarisation of $800nm$ optical probe beam in the LN film.

4 Results

4.1 Optical Confinement

Tidy3D eigenmode solver is used to determine the modes in lithium niobate thin-film with various geometries. Figure 3 presents a slot waveguide with thickness $h = 500nm$, width $W = 400nm$, and slot width $Ws = 100nm$. Figures 4 presents the mode field distribution for this geometry, showing the quasi-TE (TE) and quasi-TM (TM) modes, respectively. The results indicate that for the TE mode, the optical field intensity inside the waveguide is enhanced compared to standard lithium niobate waveguides, while the effective mode area is reduced.

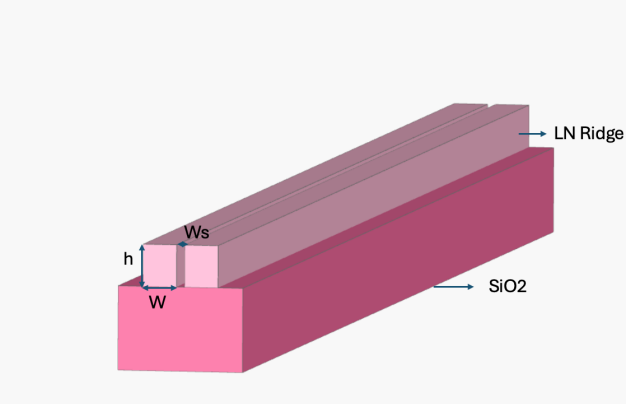

Figure 3: Structure of lithium niobate thin film slot waveguide

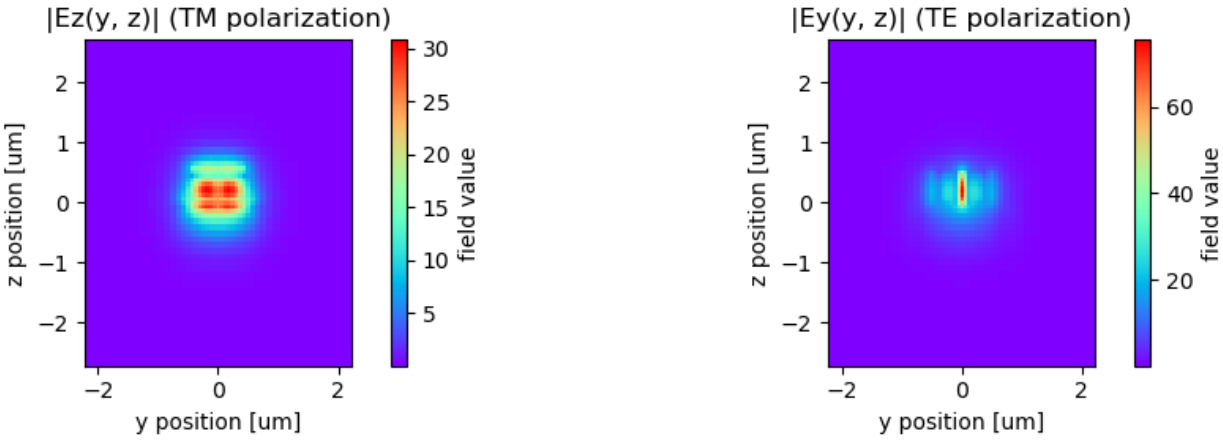

Figure 4: Slot waveguide mode distribution

Figure 5 shows the mode field distribution for a slab ridge waveguide with thickness h=500 nm, width W=400 nm, and slot width Ws=100 nm. The quasi-TE (TE) and quasi-TM (TM) modes, are represented respectively. Figure 6 shows the mode field distribution for a ridge waveguide with thickness h=500 nm, width W=400 nm. The quasi-TE (TE) and quasi-TM (TM) modes, are represented respectively.

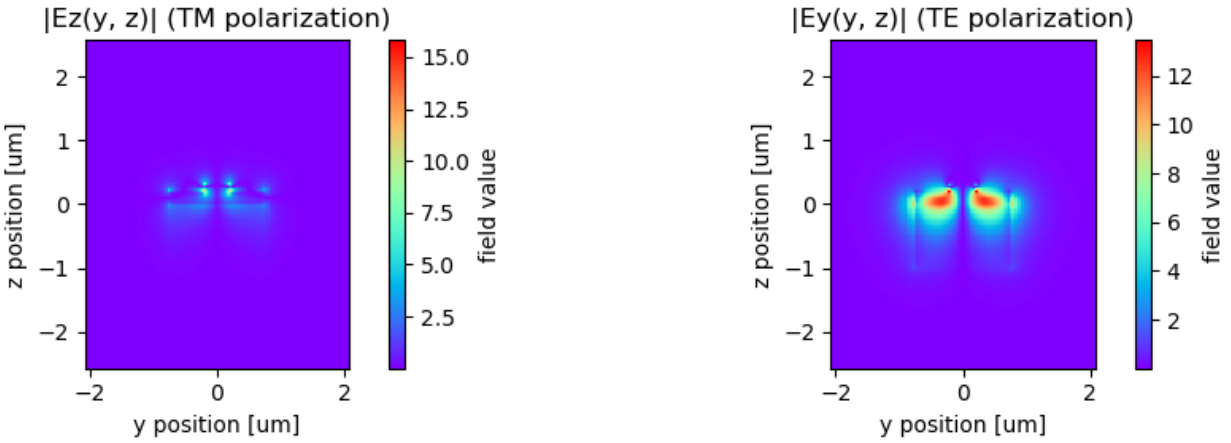

Figure 5: Slab ridge waveguide mode distribution

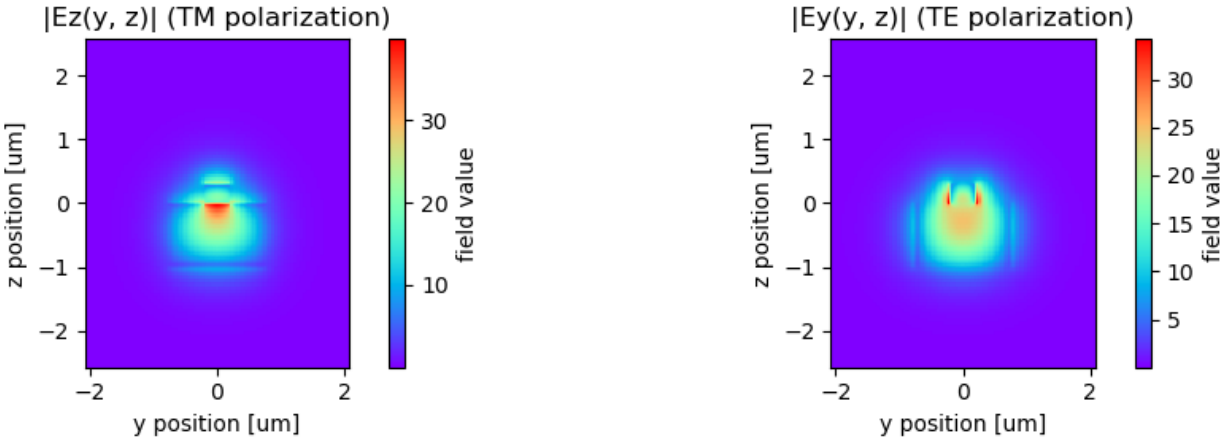

Figure 6: Ridge waveguide mode distribution

The eigenmode simulations show clear differences in confinement performance between slot, slab ridge, and ridge geometries. For the slot waveguide ($h = 500$ nm, $W = 400$ nm, $W_s = 100$ nm), the TE mode demonstrates the strongest confinement within the lithium niobate layer, with reduced mode leakage into the SiO_2 substrate. This results in a smaller effective mode area and stronger overlap with the active material, which directly enhances electro-optic efficiency.

Comparisons with the slab ridge and ridge geometries indicate that while confinement is still present, leakage into the cladding and substrate is more pronounced. For the ridge waveguide, confinement is less efficient, particularly for the TM mode, where field distribution extends significantly into the substrate. These results support the conclusion that slot geometries provide the most favourable conditions for maximizing the overlap integral between the optical and THz fields.

As shown in the figures, slot waveguides exhibit best confinement of TE modes in general. Subsequently, the effective refractive index of lithium niobate for various geometries under $800nm$ probe beam is calculated from the simulation results. The impact of width (W), slot width (Ws), and height (h) are examined. The results of the analysis are presented in Figure 7a and 7b.

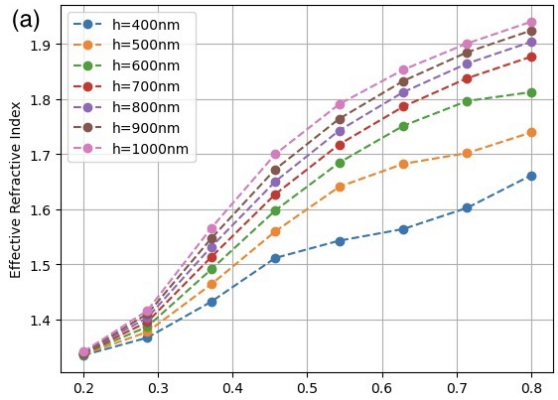

(a) Effective index n_{eff} against width W, showing variation of effective refractive index with respect to slot height, h

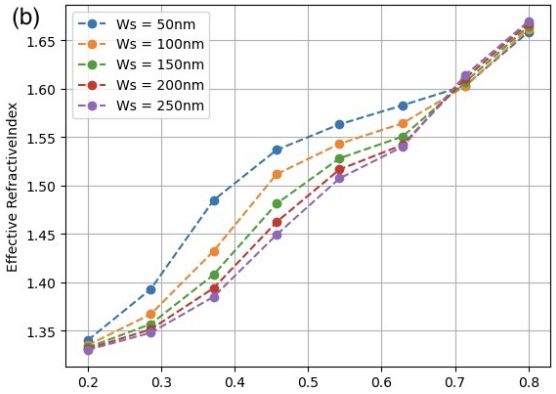

(b) Effective index n_{eff} against width W, showing variation of effective refractive index with respect to slot gap width, W_s

Figure 7: Optical confinement performance for various geometries

The parametric sweeps of height (h) and slot width (W_s) further highlight sensitivity to geometric parameters. As h increases, the effective refractive index rises, improving confinement but also potentially shifting phase-matching conditions. Conversely, increasing W_s reduces the effective index by broadening the field distribution, thereby decreasing confinement. This trade-off underscores the need to carefully balance optical confinement with phase matching when selecting waveguide dimensions.

4.2 Cherenkov plots

Cherenkov angle β was calculated as a function of the effective refractive index under varying geometries. Initial results suggest that for ridge geometries, β increases monotonically with waveguide thickness, while slot geometries exhibit a more gradual variation, enabling finer control over phase matching. Importantly, the slot waveguide configuration not only enhances confinement but also offers tunability of the Cherenkov angle, supporting simultaneous optimization of confinement and phase matching.

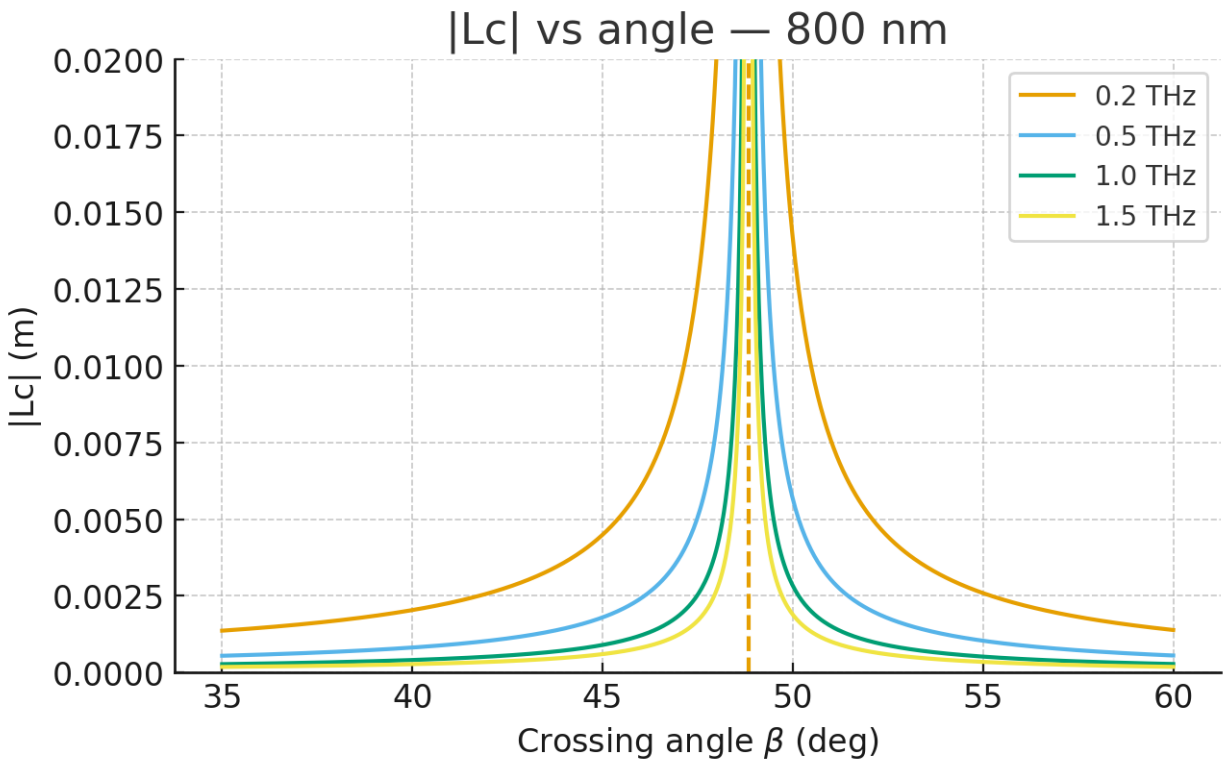

Figure 8: Enter Caption

Phase-matching quality is quantified using the coherence length

$$L_c = \frac{\pi}{|\Delta k|} \tag{3}$$

where $\Delta k = k_{\text{opt}} - k_{\text{THz}} \cos\beta$ and $k_{\text{opt}} = \frac{2\pi}{\lambda_0} n_{\text{eff}}(\lambda_0)$ is the optical propagation constant at $\lambda_0 = 800$ nm, and $k_{\text{THz}} = \frac{2\pi}{\lambda_{\text{THz}}} n_{\text{THz}}(\Omega)$ is the THz propagation constant in the substrate at angular frequency Ω. The Cherenkov angle β follows the kinematic relation

$$\cos\beta(\Omega) = \frac{v_{\text{opt}}}{v_{\text{THz}}} = \frac{n_{\text{eff}}(\lambda_0)}{n_{\text{THz}}(\Omega)}.$$

In the plotted $L_c(\beta)$ curves, a sharp rise in L_c appears as β approaches the phase-matching angle β_{pm} where $\Delta k \to 0$. Around β_{pm}, small angular changes produce large variations in L_c, highlighting both the performance benefit (long interaction length for weak-signal detection) and the sensitivity to fabrication tolerances and alignment.

Because $n_{\text{eff}}(\lambda_0)$ is geometry-dependent, varying film thickness h, ridge/slot width W, and slot gap W_s shifts k_{opt} and therefore β_{pm}. Geometries that improve confinement, for example, narrower slots or larger h, generally increase cherenkov angles to larger values and steepen the peak $L_c(\beta)$. Slot waveguides tend to

yield a broader, slightly flatter apex than simple ridges, offering a wider "high-L_c" operating window while preserving strong confinement.

As shown in figure 9, there exists a clear dependence of the Cherenkov angle β on both waveguide height h and slot width W_s, reflecting the strong influence of geometry on the effective refractive index. In general, increasing h strengthens optical confinement, raises n_{eff}, and thus reduces β, while increasing W_s weakens confinement, lowers n_{eff}, and leads to larger β. This tunability is advantageous for waveguide design, as it allows β to be engineered towards values compatible with practical collection geometries and detector layouts. Importantly, the plots also highlight the presence of regions where β changes only gradually with geometry, corresponding to flatter $L_c(\beta)$ plateaus. Such regions are especially desirable because they combine long coherence length with improved fabrication tolerance and alignment robustness. These results confirm that appropriate control of (h, W_s) provides a direct handle on optimizing both electro-optic interaction strength and practical device yield.

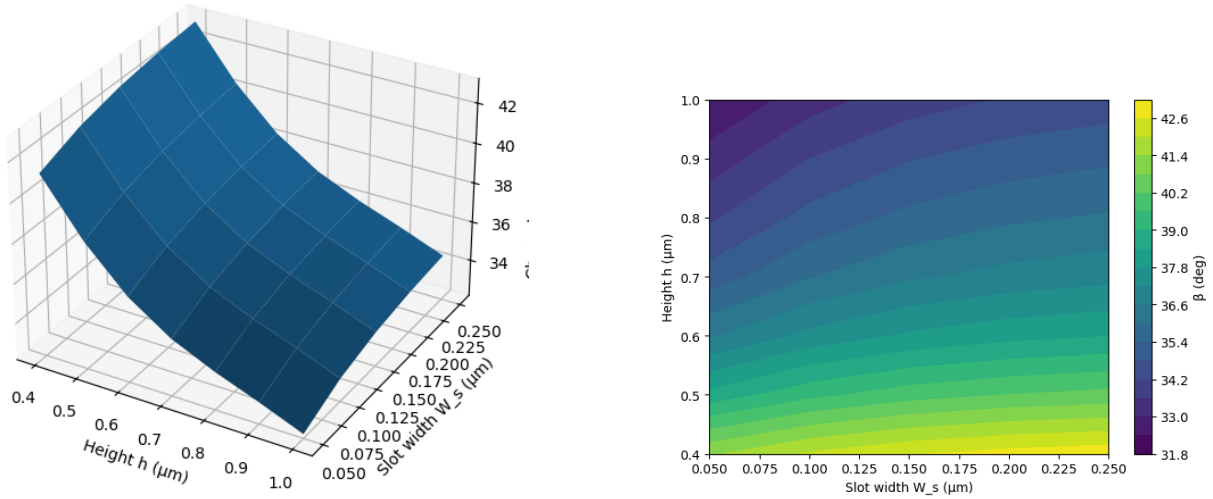

(a) 3D variation plot

(b) 2D variation plot

Figure 9: $\beta(h, W_s)$ at fixed ridge width W^*

5 Conclusion

This study investigated geometry optimization of thin-film LNOI terahertz waveguides with the aim of improving detection efficiency for healthcare-oriented THz sensing. Through systematic simulations, we demonstrated that detector geometry plays a decisive role in balancing optical confinement and phase matching, both of which are critical for enhancing electro-optic interaction strength. Slot waveguides were found to provide superior optical confinement compared to ridge and slab ridge configurations, concentrating the optical field within the lithium niobate layer and minimizing leakage into the substrate. This enhanced confinement directly improves overlap with the terahertz field, leading to higher sensitivity. Phase matching analysis using Cherenkov geometry further highlighted the importance of precise dimensional control. Adjustments in waveguide height and slot width were shown to significantly affect the effective refractive index, thereby tuning the Cherenkov angle and coherence length. Importantly, slot geometries not only allowed stronger confinement but also enabled a broader operational window with longer coherence lengths and improved tolerance to fabrication imperfections. This dual benefit suggests that carefully engineered slot waveguides represent a promising path toward robust and efficient electrode-less LNOI detectors. Overall, the findings reinforce the value of geometry-driven design in advancing THz sensing technology. By optimizing confinement and phase matching simultaneously, the proposed structures address the limitations of weak-signal detection in air-sensitive terahertz systems. Future work should expand into experimental validation of the optimized geometries, integration with collection optics, and assessment under realistic operating conditions, including biological samples. These steps would bring LNOI-based terahertz detectors closer to deployment in practical diagnostic platforms, supporting the development of rapid and non-invasive healthcare screening tools.

References

[1] N. Akter, M. M. Hasan, and N. Pala. "A Review of THz Technologies for Rapid Sensing and Detection of Viruses including SARS-CoV-2". In: *Biosensors* 11.10 (Sept. 2021), p. 349. DOI: 10.3390/bios11100349.

[2] Xueping Chen et al. "Label-free techniques for laboratory medicine applications". In: *Frontiers in Laboratory Medicine* 1.2 (2017), pp. 82–85. DOI: 10.1016/j.flm.2017.05.004.

[3] C. Gutiérrez-Martínez et al. "Modeling and experimental electro-optic response of dielectric lithium niobate waveguides used as electric field sensors". In: *Measurement Science and Technology* 22.3 (2011), p. 035207. DOI: 10.1088/0957-0233/22/3/035207.

[4] Jianjun Ma et al. "Terahertz channels in atmospheric conditions: Propagation characteristics and security performance". In: *Fundamental Research* (2024). DOI: 10.1016/j.fmre.2024.01.001.

[5] I. Wilke, J. Monahan, S. Toroghi, et al. "Thin-film lithium niobate electro-optic terahertz wave detector". In: *Scientific Reports* 14 (2024), p. 4822. DOI: 10.1038/s41598-024-49700-y.